Applied Catalysis B: Environmental 234 (2018) 50–55

Contents lists available at ScienceDirect

Applied Catalysis B: Environmental

journal homepage: www.elsevier.com/locate/apcatb

Photocatalytic splitting of thiols to produce disulfides and hydrogen over $PtS/ZnIn_2S_4$ nanocomposites under visible light

Lizhi Xu, Xiaoyu Deng, Zhaohui Li*

Research Institute of Photocatalysis, State Key Laboratory of Photocatalysis on Energy and Environment, College of Chemistry, Fuzhou University, Fuzhou, 350116, PR China

ARTICLE INFO

Keywords:
Photocatalytic
$PtS/ZnIn_2S_4$
Hydrogen
Thiols splitting
Visible light

ABSTRACT

Photoreduction of $[PtCl_6]^{2-}$ over hexagonal $ZnIn_2S_4$ led to the formation of surface deposited small PtS nanoparticles with a size of ca. 3 nm. The resultant $PtS/ZnIn_2S_4$ nanocomposites were fully characterized and their performance for photocatalytic splitting of thiols to produce disulfides and hydrogen was investigated. It was found that PtS significantly promoted the photocatalytic performance for thiols splitting to produce disulfides and quantitative hydrogen over $ZnIn_2S_4$ under visible light and no over-oxidized products of thiols were produced. An optimum performance was observed over 0.5 wt% $PtS/ZnIn_2S_4$, with a complete transformation of thiols to disulfides in 6 h. $PtS/ZnIn_2S_4$ nanocomposite is stable during the photocatalytic reaction and can be easily separated for recycling. The photocatalytic thiols splitting over $PtS/ZnIn_2S_4$ is an efficient and cost effective strategy to produce disulfides, which exhibits 100% atom economy since hydrogen is generated concomitantly. This study demonstrates that the coupling of water reduction with organics oxidation over semiconductor-based photocatalysts may find great potentials in organic syntheses.

1. Introduction

The synthesis of disulfides has received extensive attention due to their indispensable roles in many important synthetic chemistry, biochemistry and industrial applications. The most common approach for the synthesis of disulfides is the oxidative coupling using stoichiometric oxidants or catalytic oxidation of thiols, since a number of thiols are commercially available or can be easily synthesized. However, over-oxidation of thiols to generate undesirable sulfoxides, sulfones, thiosulfinates or thiosulfonates as byproducts during the syntheses of disulfides from thiols occurs and therefore complicated purification processes are usually required [1,2]. In addition, sometimes hazardous chemicals and expensive metal containing reagents or catalysts are also involved [3–5].

With an effort to develop green and sustainable chemistry, recently researchers are paying increasing interest in the light-driven organic syntheses [6–10]. The use of light to trigger the transformation of thiols to produce disulfides is interesting considering that light has the unique capability of spatial control, which can induce reactions locally via delivering light to a specific area of interest, a capability especially important in biochemistry and catalysis. In 2010, Yoon et al. first reported that some light excitable aromatic thiols undergo photooxidative couplings to produce disulfides without the requirement of a catalyst [11]. However, the substrate scope for this protocol is limited. The coupling of thiols to produce disulfides with concomitant generation of hydrogen was for the first time realized over a homogeneous [$Mn(CO)_5Br$] complex as the photosensitizer under UV irradiation [12]. More recently, Wu and co-workers reported that excellent conversion of thiols and high TON for the generation of disulfides can be achieved over CdSe QDs as photocatalyst using a high power Hg lamp [13]. As compared with the homogeneous catalysts, heterogeneous photocatalysts may provide more advantages in catalyst separation for recycling. Recently, heterogeneous photocatalysts GO-FePc (Pc = phthalocyanine) and CoOx-C,N@CeO_2 were also used in the oxidative coupling of thiols to produce disulfides using O_2 as oxidant [14,15]. Considering the atom efficiency, it is more desirable that the thiols can directly split to produce disulfides with concomitant generation of hydrogen.

Hexagonal $ZnIn_2S_4$ is a chalcogenide semiconductor that has a band gap corresponding to visible-light absorption as well as suitable band positions, with the top of its valance band located at 1.37 eV versus NHE, while the bottom of the conduction band located at –0.73 eV versus NHE [16]. $ZnIn_2S_4$ has been extensively studied for a series of photocatalytic applications under visible light [17–20]. When coupled with co-catalysts like Pt [21], MoS_2 [22,23], NiS [24] and RGO [25,26] to provide active sites and to lower the over potential for hydrogen

* Corresponding author.
E-mail address: zhaohuili@fzu.edu.cn (Z. Li).

https://doi.org/10.1016/j.apcatb.2018.04.030
Received 8 February 2018; Received in revised form 22 March 2018; Accepted 16 April 2018
Available online 17 April 2018
0926-3373/

generation, $ZnIn_2S_4$ exhibit superior photocatalytic activity for hydrogen evolution in the presence of sacrificial agents like Na_2S/Na_2SO_3, TEA and TEOA [27–32].

Considering that thiols are also good electron donors and hydrogen sources, it is therefore interesting to investigate the photocatalytic splitting of thiols to form disulfides with the concomitant generation of hydrogen over $ZnIn_2S_4$. In this manuscript, we reported the deposition of PtS as a co-catalyst on the surface of $ZnIn_2S_4$ via a photo reduction process. The performance of the resultant PtS/$ZnIn_2S_4$ nanocomposites for photocatalytic splitting of thiols was investigated. Previous studies have revealed that metal chalcogenides like MoS_2 [33,34], WS_2 [35,36], NiS [37–39] and CoS [40,41] are active cocatalysts for photocatalytic H_2 evolution. It was found that PtS also acts as an efficient cocatalyst to promote photocatalytic thiols splitting to generate disulfides and quantitative hydrogen over $ZnIn_2S_4$ under visible light. This study not only provides an efficient, cost effective strategy for the production of disulfides, but also highlights the great potential of using semiconductor-based photocatalysts for light-driven organic syntheses by coupling with H_2O reduction to generate hydrogen.

2. Experimental

2.1. Preparations

All the reagents are analytical grade and used without further purifications. Hexagonal $ZnIn_2S_4$ was synthesized according to our previously reported method [42]. PtS/$ZnIn_2S_4$ nanocomposites were prepared via a photoreduction process. Typically, $ZnIn_2S_4$ (200 mg) was suspended in CH_3OH solution (3 mL) containing different amount of H_2PtCl_6. The resultant suspension was stirred under N_2 atmosphere for 30 min and irradiated with a 300 W Xe lamp. After illuminated for 3 h, the resultant products were filtered, washed with de-ionized water and dried overnight at 60 °C in oven. PtS/$ZnIn_2S_4$ nanocomposites with different amount of PtS were denoted as x wt% PtS/$ZnIn_2S_4$. For comparison, 1.0 wt% Pd/$ZnIn_2S_4$, 1.0 wt% NiS/$ZnIn_2S_4$ and 1.0 wt% MoS_2/$ZnIn_2S_4$ were prepared following the procedure reported previous [24,34].

2.2. Characterizations

X-ray diffraction (XRD) patterns were collected on a Rigaku Miniflex 600 X-ray diffractometer with Cu K_α radiation. X-ray photoelectron spectroscopy (XPS) measurements were performed on a PHI Quantum 2000 XPS system with a monochromatic Al K_α source and a charge neutralizer. All the binding energies were referred to the C 1 s peak at 284.6 eV of the surface adventitious carbon. The morphology of the sample was studied by a field emission scanning electron microscopy (SEM) (JSM-6700F). The transmission electron microscopy (TEM) and high-resolution transmission electron microscopy (HRTEM) images were measured using a JEOL model JEM 2010 EX instrument at an accelerating voltage of 200 kV. The powder particles were supported on a carbon film coated on a 3 mm diameter fine-mesh copper grid. A suspension of the sample in ethanol was sonicated and a drop was dripped on the support film. UV–vis diffraction spectra (UV–vis DRS) of the powders were obtained for the dry pressed disk samples using a UV–vis spectra photometer (Cary 500 Scan Spectrophotometers, Varian). $BaSO_4$ was used as a reflectance standard.

2.3. Photocatalytic reactions

The photocatalytic splitting of thiols to produce disulfides and hydrogen was performed in a schlenk tube. 5 mg of photocatalyst was evacuated and purged with N_2 for several times. A mixed solution of CH_3CN and H_2O in 3:1 (v/v) (2 ml) containing thiols (0.1 m mol) was pre-degassed with N_2 to remove any dissolved O_2 and was injected into the above schlenk tube. The suspension was irradiated with a 5 W LED lamp (Light-emitting diodes, PCX50A, multichannel optical catalytic reaction system) with a wavelength centered at 450 nm. After reaction, the gaseous products were analyzed by GC-TCD (Shimadzu GC-2014) with a TDX-01 packed column. The filtrate was extracted with ethyl acetate for three times and was analyzed by GC-FID (Shimadzu GC-2014) equipped with a HP-5 capillary column. The apparent quantum yields (AQYs) for hydrogen evolution over 0.5 wt% PtS/$ZnIn_2S_4$ was measured under the same photocatalytic reaction condition except that a band pass filter centered at 420 nm was used. The AQYs for photocatalytic hydrogen production were represented as AQY % = (2 × number of hydrogen molecules formed) / (number of incident photons) × 100%.

3. Results and discussion

$ZnIn_2S_4$ was prepared according to our previously reported method, and different amounts of PtS were loaded on $ZnIn_2S_4$ by a photoreduction process. The XRD patterns of all the obtained products show 2θ peaks at values of 14.3, 21.2, 27.7, 30.4, 39.3, 47.5, 52.1, 55.8 and 76.4°, which can be assigned to (004), (006), (102), (104),(108), (110), (116), (022) and (123) crystallographic planes of hexagonal $ZnIn_2S_4$ phase (JCPDS 03-065-2023) (Fig. 1). No diffractions peaks corresponding to metallic Pt or Pt-containing compounds are observed in the XRD patterns of the products, probably due to the low amount of introduced Pt or the overlap of their diffractions peaks with those of hexagonal $ZnIn_2S_4$. However, the existence of Pt in the as-prepared products was confirmed by the XPS. The high resolution XPS spectra of the product in the Pt 4f region shows two peaks at 75.66 and 72.23 eV, which indicates that Pt exists as Pt^{2+} in the nanocomposite (Fig. 2a). The XPS spectra in S 2p region can be deconvoluted into two sets of peaks, indicating that S exists in two different chemical environments (Fig. 2b). Considering that Pt exists as Pt^{2+} and by comparison with pure $ZnIn_2S_4$, the peak at 161.39 and 162.64 eV can be assigned to S $2p_{3/2}$ and S $2p_{1/2}$ in $ZnIn_2S_4$, while the other two peaks at 160.84 and 162.08 eV can be assigned to S $2p_{3/2}$ and S $2p_{1/2}$ in PtS, respectively. It is known that the conduction band of hexagonal $ZnIn_2S_4$ located at –0.73 eV vs NHE, which is negative than E($PtCl_6^{2-}$/Pt^{2+}) (0.21 V vs NHE). Therefore during the photoreduction process, the photogenerated electrons in $ZnIn_2S_4$ can reduce $PtCl_6^{2-}$ to surface adsorbed Pt^{2+}, which can further react with S^{2-} to form PtS, while CH_3OH act as sacrificial electron donor to consume the left photogenerated holes in $ZnIn_2S_4$ and complete the photocatalytic cycle. The photoreduction of $PtCl_6^{2-}$ over $ZnIn_2S_4$ to form surface deposited PtS for photocatalytic hydrogen evolution has also been reported previously [43]. The high resolution XPS spectra show peaks at 1021.65 and 1044.8 eV for Zn $2p_{3/2}$ and Zn $2p_{1/2}$, while peaks at 444.61 and 452.17 eV correspond to In $3d_{5/2}$ and In $3d_{3/2}$ (Fig. 2c and d). In comparison with those in bare $ZnIn_2S_4$ (Fig. S1), both the Zn 2p peaks and In 3d peaks in PtS/$ZnIn_2S_4$

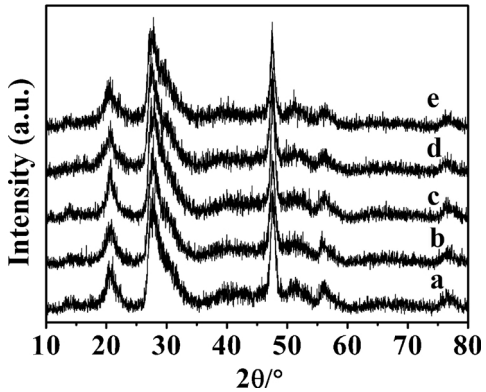

Fig. 1. Powder XRD of (a) $ZnIn_2S_4$; (b) 0.1 wt% PtS/$ZnIn_2S_4$; (c) 0.2 wt% PtS/$ZnIn_2S_4$; (d) 0.5 wt% PtS/$ZnIn_2S_4$; (e)1.0 wt% PtS/$ZnIn_2S_4$.